Description of Gloeomargarita lithophora gen. nov., sp. nov., a thylakoid-bearing, basal-branching cyanobacterium with intracellular carbonates, and proposal for Gloeomargaritales ord. nov.

David Moreira, Rosaluz Tavera, Karim Benzerara, Fériel Skouri-Panet, Estelle Couradeau, Emmanuelle Gérard, Céline Loussert Fonta, Eberto Novelo, Yvan Zivanovic, Purificación López-García

International Journal of Systematic and Evolutionary Microbiology

Description of Gloeomargarita lithophora gen. nov., sp. nov., a thylakoid-bearing basal-branching cyanobacterium with intracellular carbonates, and proposal for Gloeomargaritales ord. nov.

--Manuscript Draft--

Manuscript Number:	IJSEM-D-16-00670R2
Full Title:	Description of Gloeomargarita lithophora gen. nov., sp. nov., a thylakoid-bearing basal-branching cyanobacterium with intracellular carbonates, and proposal for Gloeomargaritales ord. nov.
Article Type:	Note
Section/Category:	New taxa - other bacteria
Keywords:	Gloeomargarita; cyanobacteria, phylogeny.
Corresponding Author:	David Moreira Centre National de la Recherche Scientifique FRANCE
First Author:	David Moreira
Order of Authors:	David Moreira
	Rosaluz Tavera
	Karim Benzerara
	Fériel Skouri-Panet
	Estelle Couradeau
	Emmanuelle Gérard
	Céline Loussert Fonta
	Eberto Novelo
	Yvan Zivanovic
	Purificación López-García
Manuscript Region of Origin:	FRANCE
Abstract:	A unicellular cyanobacterium, strain Alchichica-D10, was isolated from microbialites of the alkaline Lake Alchichica, Mexico. The cells were short rods (3.9 ± 0.6 µm in length and 1.1 ± 0.1 µm in width) forming biofilms of intense emerald green color. They exhibited red autofluorescence under UV light excitation. UV-visible absorption spectra revealed that they contain chlorophyll a and phycocyanin, and electron microscopy showed the presence of thylakoids. The strain grew within a temperature range of 15-30 °C. Genomic DNA G+C content was 52.2 mol%. The most remarkable feature of this species was its granular cytoplasm, due to the presence of numerous intracellular spherical granules (16-26 per cell) with an average diameter of 270 nm. These granules, easily visible under scanning electron microscopy, were composed of amorphous carbonate containing Ca, Mg, Ba, and Sr. A multi-gene phylogeny based on the analysis of 59 conserved protein markers supported robustly that this strain occupies a deep position in the cyanobacterial tree. Based on its phenotypic characters and phylogenetic position, strain Alchichica-D10 is considered to represent a new genus and novel species of cyanobacteria for which the name Gloeomargarita lithophora gen. nov., sp. nov. is proposed. The type strain is Alchichica-D10 (Culture Collection of Algae and Protozoa CCAP strain 1437/1; Collections de Cyanobactéries et Microalgues Vivantes of the Museum National d'Histoire Naturelle in Paris strain PMC 919.15). Furthermore, a new family, Gloeomargaritaceae, and a new order, Gloeoemargaritales, are proposed to accommodate this species under the International Code of Nomenclature for algae, fungi, and plants.

Description of *Gloeomargarita lithophora* gen. nov., sp. nov., a thylakoid-bearing basal-branching cyanobacterium with intracellular carbonates, and proposal for *Gloeomargaritales* ord. nov.

David Moreira,[1] Rosaluz Tavera,[2] Karim Benzerara,[3] Fériel Skouri-Panet,[3] Estelle Couradeau,[1,2*] Emmanuelle Gérard,[4] Céline Loussert Fonta,[5] Eberto Novelo,[2] Yvan Zivanovic[6] and Purificación López-García[5]

[1]Unité d'Ecologie, Systématique et Evolution, CNRS UMR 8079, Université Paris-Sud/Paris-Saclay, AgroParisTech, 91400 Orsay, France

[2]Facultad de Ciencias, Universidad Nacional Autónoma de México, CDMX, México

[3]Institut de Minéralogie, de Physique des Matériaux, et de Cosmochimie, Sorbonne Universités - UPMC Univ Paris 06, CNRS UMR 7590, MNHN, IRD UMR 206 Paris, France

[4]Géobiosphère Actuelle et Primitive, Institut de Physique du Globe de Paris, CNRS UMR 7154, Université Paris Diderot, Sorbonne Paris Cité, Paris, France

[5]Nestlé Research Center, Minerals and Imaging Group, P.O Box 44, Ch-1000 Lausanne 26, VD, Switzerland

[6]Institut de Génétique et Microbiologie, CNRS UMR 8621, Université Paris-Sud/Paris-Saclay, 91405 Orsay, France

[*]Now in School of Life Sciences, Arizona State University, Tempe, AZ 85287, USA

Correspondence
David Moreira
David.moreira@u-psud.fr

Running title: *Gloeomargarita lithophora* gen. nov., sp. nov.

Contents category: New Taxa (Other Bacteria).

The GenBank accession number for the sequences of 59 conserved genes of strain Alchichica-D10 is CP017675.

A unicellular cyanobacterium, strain Alchichica-D10, was isolated from microbialites of the alkaline Lake Alchichica, Mexico. The cells were short rods (3.9 ± 0.6 μm in length and 1.1 ± 0.1 μm in width) forming biofilms of intense emerald green color. They exhibited red autofluorescence under UV light excitation. UV-visible absorption spectra revealed that they contain chlorophyll *a* and phycocyanin, and electron microscopy showed the presence of thylakoids. The strain grew within a temperature range of 15-30 °C. Genomic DNA G+C content was 52.2 mol%. The most remarkable feature of this species was its granular cytoplasm, due to the presence of numerous intracellular spherical granules (16-26 per cell) with an average diameter of 270 nm. These granules, easily visible under scanning electron microscopy, were composed of amorphous carbonate containing Ca, Mg, Ba, and Sr. A multi-gene phylogeny based on the analysis of 59 conserved protein markers supported robustly that this strain occupies a deep position in the cyanobacterial tree. Based on its phenotypic characters and phylogenetic position, strain Alchichica-D10 is considered to represent a new genus and novel species of cyanobacteria for which the name *Gloeomargarita lithophora* gen. nov., sp. nov. is proposed. The type strain is Alchichica-D10 (Culture Collection of Algae and Protozoa CCAP strain 1437/1; Collections de Cyanobactéries et Microalgues Vivantes of the Museum National d'Histoire Naturelle in Paris strain PMC 919.15). Furthermore, a new family, *Gloeomargaritaceae*, and a new order, *Gloeoemargaritales*, are proposed to accommodate this species under the International Code of Nomenclature for algae, fungi, and plants.

Cyanobacteria thrive in a variety of aquatic and terrestrial habitats, where their ability, unique among bacteria, to carry out oxygenic photosynthesis makes them ecologically significant (Castenholz, 2001). They are also important from an evolutionary point of view since they were responsible for the early oxygenation of the Earth's atmosphere (Buick, 2008) and an ancestral cyanobacterium was the endosymbiont that gave rise to the chloroplasts now found in eukaryotic algae and plants (Gray & Doolittle, 1982). In addition, cyanobacteria have a rich fossil record. The massive fossil stromatolites dating back to at least 2.7 billion years ago are considered to have been built by microbial communities dominated by cyanobacteria (Altermann *et al.*, 2006) and unequivocal calcified cyanobacterial fossils are common since the base of the early Cambrian, with *Girvanella* as the first undisputed occurrence at 700 million years ago (Riding, 2006). The capacity of several cyanobacteria to precipitate calcium carbonate may have enhanced their preservation and explain, at least partly, their extensive

fossil record. In fact, several species induce calcium carbonate precipitation by their photosynthetic activity (Arp *et al.*, 2001; Kamennaya *et al.*, 2012), which increases locally the concentration of CO_3^{2-} by the disproportionation of HCO_3^- to CO_3^{2-} and CO_2, the latter being fixed by the enzyme ribulose-1,5-bisphosphate carboxylase-oxygenase (RuBisCO). The export of alkalinity from the intracellular to the extracellular medium, by a mechanism that remains poorly known, raises the saturation index for carbonate minerals in the immediate cell environment and thus leads to mineral precipitation if free cations (e.g., Ca^{2+}) and nucleation sites are present. It has also been proposed that the cell surface, in particular the exopolysaccharidic matrix, may serve as a nucleation site for carbonates (Obst *et al.*, 2009). In all cases, the precipitation of carbonates by cyanobacteria has been regarded as an extracellular uncontrolled process.

However, we recently reported the discovery of a cyanobacterial species that contained intracellular carbonate inclusions (Couradeau *et al.*, 2012). It was the first time that this capacity was found in cyanobacteria. More recently, this capability has also been found in a small number of other cyanobacterial taxa (Benzerara *et al.*, 2014; Li *et al.*, 2016). Intracellular carbonates appear to be generally rare in bacteria since, up to the recent discovery in cyanobacteria, their occurrence had been described only in a single species, the proteobacterium *Achromatium oxaliferum* (Head *et al.*, 1996). The new cyanobacterial strain Alchichica-D10, which we provisionally named *Candidatus* Gloeomargarita lithophora (Couradeau *et al.*, 2012), was isolated from microbialite samples collected in the alkaline (~43 mM HCO_3^-, pH ~8.9) Lake Alchichica (Mexico) in 2007 and maintained alive in laboratory aquaria since then. Here, we describe formally this new species and its phylogenetic position within the Cyanobacteria.

Lake Alchichica microbialites are mostly composed of hydromagnesite [$Mg_5(CO_3)_4(OH)_2$•$4(H_2O)$] and aragonite ($CaCO_3$), and the microbial community inhabiting them is largely dominated by very diverse cyanobacteria (Couradeau *et al.*, 2011; Saghai *et al.*, 2015). After several years of growth in laboratory aquaria, the microbialites collected in 2007 were still inhabited by a large diversity of cyanobacteria similar to that found in the Lake, which suggests that this community is highly resilient (Couradeau *et al.*, 2011). Microbialites and the aquaria walls were covered by extensive biofilms. These biofilms contained different cyanobacterial morphotypes, with a particularly abundant one consisting of small rod-shaped cells with granular cytoplasm, noticeable under optical microscopy (Fig. 1). To enrich this cyanobacterial species, we disrupted a biofilm sample and filtered the

detached cells through an isopore filter of 3 µm pore size. We then inoculated a 96-well plate containing BG11 medium with the filtered cells. After one month of incubation at 21 °C applying a diel cycle, we observed growth of the targeted morphotype in 6 wells. Sequencing of the 16S rRNA gene from these 6 cultures yielded identical sequences (Couradeau *et al.*, 2012; accession number JQ733894). We further purified this cyanobacterium by growth on BG11-agar plates and single colony isolation. This allowed us to obtain cultures with this single cyanobacterial species. However, sequencing of 16S rRNA genes amplified with universal bacterial primers revealed the presence of a contaminant alphaproteobacterium closely related to several species of the genus *Sandarakinorhabdus* (with 97% 16S rRNA gene sequence similarity). We have been unable to eliminate this contaminant from our cultures, partly due to the very slow growth rate of the cyanobacterium. Interestingly, some of these *Sandarakinorhabdus* species have also been reported in association with other cyanobacteria, such as the strain *Sandarakinorhabdus* sp. A14 that is found in cultures of *Microcystis aeruginosa* (Shi *et al.*, 2009). Nevertheless, observations using epifluorescent optical microscopy and scanning electron microscopy (SEM) showed that the cultures were largely dominated by the cyanobacterium and that the contaminant appeared to be rare. Thus, even if non-axenic, the cultures were suitable for the description of the new cyanobacterial species using a variety of techniques.

Cyanobacterial cells belonging to the new Alchichica-D10 strain grown in BG11 medium measured 3.9 ± 0.6 µm in length and 1.1 ± 0.1 µm in width. The most conspicuous feature of those cells observed under SEM (using secondary electron mode) was the presence of numerous bright intracellular spherical granules (3-19 per cell) measuring between 60 and 380 nm in diameter (Fig. 2a). As previously determined by Benzerara *et al.* (2014) using energy-dispersive x-ray spectrometry (EDXS), these inclusions were composed of Ca carbonate. In addition, cells grown in BG11 contained a relatively small number of larger and darker inclusions rich in P that corresponded to polyphosphate granules (Fig. 2b). When grown in the aquarium water, highly alkaline and rich in Ca, Mg, and other cations but poor in P, the cells contained more carbonate granules (16 to 26 per cell) with an average diameter of 270 nm. In contrast with cells grown in BG11, the chemical composition of these inclusions contained Mg, Ba, and Sr as major elements in addition to Ca, and polyphosphate granules were rare (Fig. S1, available in the online Supplementary Material). Interestingly, Ba/Ca and Sr/Ca atomic ratios in the inclusions were 1370 and 86 times higher, respectively, than those measured in the aquaria solution (Couradeau *et al.*, 2012), although Ca, Sr and Ba are usually

supposed to be incorporated relatively conservatively by carbonates. This suggested that the cells controlled the chemical composition of the inclusions.

The ultrastructure of the cells was studied by transmission electron microscopy (TEM). In addition to the typical Gram negative double cell membrane, an important structural feature was the presence of thylakoids, clearly visible as several concentric layers parallel to the cell periphery (Fig. 3). The occurrence of thylakoids clearly differentiates *Gloeomargarita lithophora* from the deep-branching genus *Gloeobacter*, which lacks these endomembrane structures (Rippka *et al.*, 1974). Intracellular structures were observed in the same cells with a contrast different from that of carbonate or polyphosphate inclusions (see arrows in Fig. 3) but with morphological and contrast similarities with carboxysomes found in other cyanobacteria (e.g., Porta *et al.*, 2000).

Cells observed by confocal laser scanning microscopy (CLSM) under UV light (405 nm) excitation showed intense red autofluorescence (Fig. S2, available in the online Supplementary Material). The absorption spectrum of pigments extracted with 90% acetone showed peaks at wavelengths of 620 and 664 nm, indicating the presence of phycocyanin and chlorophyll *a* (Fig. S3, available in the online Supplementary Material), which are typical pigments of cyanobacteria.

Strain Alchichica-D10 colonies grew very slowly on agar plates. They exhibited an intense emerald color and were surrounded by a thick mucilaginous cover (Fig. S4a, available in the online Supplementary Material). Individual cells appear to be able to glide on the plate surface to initiate the growth of new peripheral colonies (Fig. S4b, available in the online Supplementary Material). This phenomenon can lead to the formation of migration fronts that provide a stratified structure to the margins of mature colonies (Fig. S4a, available in the online Supplementary Material). To determine the optimal growth conditions in the laboratory, we combined 3 different buffered pH values (8.0, 8.5, and 9.0), 5 temperatures (15, 20, 25, 30, and 37 °C), and 3 light intensities (photon flux of 5, 10, and 41 µmoles $m^{-2}s^{-1}$) in both liquid and solid BG11 media buffered with HEPES. Growth was extremely slow at 15° C and did not occur at 37 °C. Thus, we focused on the intermediate temperatures. In all cases, growth was slow and took at least 6 weeks to become noticeable by the development of visible colonies on solid medium or by the appearance of green color in the liquid cultures. In these liquid cultures, the highest cell densities were observed at pH 8.0 and 8.5 at 25 and 30 °C, whereas in solid medium the optimal condition appeared to be at a pH of 8.5 with low

light intensity (photon flux of 5-10 µmoles $m^{-2}s^{-1}$) and a temperature of 25-30 °C (Fig. S5, available in the online Supplementary Material).

Preliminary phylogenetic analyses based on 16S rRNA gene sequences suggested the proximity of strain Alchichica-D10 to the basal order Gloeobacterales (Couradeau *et al.*, 2012). However, this relationship was not strongly supported and was based on unrooted phylogenetic trees. In fact, a 16S rRNA rooted tree published later showed that *G. lithophora* did not branch as sister of the *Gloeobacter* species but as the second branch to diverge within the Cyanobacteria after *Gloeobacter*, though still with weak statistical support (Saw *et al.*, 2013). To resolve this uncertainty, we carried out a multi-gene phylogenetic analysis. For this purpose, we extracted *G. lithophora* genomic DNA that was sequenced using the Illumina Genome Analyzer II technology, which yielded 2.1 Gbp of DNA sequences (with a G + C content of 52.2). Among these sequences, we fetched 59 conserved genes involved in transcription and translation (Table S1, available in the online Supplementary Material). Their translated protein sequences were aligned with the respective homologous sequences found in all completely sequenced cyanobacterial genomes and several other bacteria included as outgroups. Alignments were trimmed to eliminate ambiguously aligned regions and concatenated to build a 7,220 amino acids-long concatenation, which was analyzed using Bayesian inference to reconstruct a phylogenetic tree. The resulting tree was highly supported and placed *G. lithophora* in an early-diverging position, as the third most basal cyanobacterial branch, just after the two available *Gloeobacter* species and a group containing the strain *Synechococcus* sp. PCC 7336 and the two thermophilic strains *Synechococcus* sp. JA-2-3B'a(2-13) and JA-3-3Ab isolated from Yellowstone (Fig. 4 and Fig. S6, available in the online Supplementary Material). Therefore, *Gloeobacter* and *Gloeomargarita* are not sister groups, contradicting our previous single gene-based suggestion that strain Alchichica-D10 might be a divergent species belonging to the order Gloeobacterales. Indeed, the presence of thylakoids in strain Alchichica-D10 (see above) constituted a major difference with the thylakoid-lacking *Gloeobacter* genus (Rippka *et al.*, 1974), in agreement with their placement in independent branches in the multi-gene phylogenetic tree.

Although *G. lithophora* is the only species available in culture for this new genus, a large diversity of related environmental 16S rRNA gene sequences has been detected, indicating that it belongs to a diverse clade found in various environments, in particular freshwater microbialites and microbial mats (Ragon *et al.*, 2014). Interestingly, several sequences have been retrieved from microbial mats thriving in continental hot springs from various locations,

such as Yellowstone, central Tibet, and Algeria (Amarouche-Yala *et al.*, 2014; Lau *et al.*, 2009; Turner *et al.*, 1999). Moreover, cells with morphological characteristics similar to those of *G. lithophora*, including the presence of numerous carbonate inclusions in the cytoplasm, were observed by electron microscopy in the Algerian hot spring samples (Ragon *et al.*, 2014). These results indicate that the different lineages related to *Gloeomargarita* have adapted to a wide range of temperatures.

As *G. lithophora* does not belong to the Gloeobacterales, the erection of a new genus, family and order to accommodate this new cyanobacterial species is required (see below). As far as we know, the genus name *Gloeomargarita* has never been used in botanical literature, so it can be validly published as a new cyanobacterial genus under the International Code of Nomenclature for algae, fungi and plants (McNeill *et al.*, 2012).

Description of *Gloeomargarita* gen. nov.

Gloeomargarita (Gloe.o.mar.ga.ri'ta. Gr. n. *gloios* glutinous substance; L. fem. n. *margarita* pearl; N.L. fem. n. *Gloeomargarita* glutinous cells containing pearls).

Unicellular rods with oxygenic photoautotrophic metabolism and gliding motility. Contain chlorophyll *a* and phycocyanin and photosynthetic thylakoids located peripherally. Reproduction by transverse binary fission in a single plane. Do not produce well-defined sheath layers. Contain spherical inclusions of earth alkaline carbonates in the cytoplasm. The type species is *Gloeomargarita lithophora* sp. nov.

Description of *Gloeomargarita lithophora* sp. nov.

Gloeomargarita lithophora (li.tho'pho.ra. Gr. masc. n. *lithos* stone; Gr. masc. n. *phoros* carrier; N.L. fem. n. *lithophora* carrier of stones).

Exhibits the following properties in addition to those given in the genus description. Cells are 1.1 μm wide and 3.9 μm long in average. Growth occurs at 15-30 °C (optimum 25 °C) in alkaline freshwater and BG11 medium. The G + C content of the genomic DNA of the type strain is 52.2 mol%. The type strain, Alchichica-D10 (=CCAP 1437/1, =PMC 919.15), was isolated from microbialites of the alkaline Lake Alchichica (Mexico) preserved in laboratory aquaria at Orsay (France). The 16S rRNA gene sequence of the type strain is available in GenBank under accession number JQ733894.

The holoptype of *G. lithophora* is the specimen PueAl-43a in the FCME Herbarium of the Faculty of Sciences at the UNAM. Type locality: Alchichica Lake (Mexico). Living cultures CCAP 1437/1 and PMC 919.15 are ex-holotypes.

Description of *Gloeomargaritaceae* fam. nov.

Gloeomargaritaceae (Gloe.o.mar.ga.ri.ta.ce'ae. N.L. fem. n. *Gloeomargarita* type genus of the family; suff. *–aceae* ending to denote a family; N.L. fem. pl. n. *Gloeomargaritaceae* the family of the genus *Gloeomargarita*).

The description is the same as for the genus *Gloeomargarita*.

Type genus is *Gloeomargarita* gen. nov.

Description of *Gloeomargaritales* ord. nov.

Gloeomargaritales (Gloe.o'mar.ga.ri.ta'les. N.L. fem. n. *Gloeomargarita* type genus of the order; suff. *-ales* ending denoting an order; N.L. fem. pl. n. *Gloeomargaritales* the order of the genus *Gloeomargarita*).

The description is the same as for the genus *Gloeomargarita*.

Acknowledgements

This research was funded by the European Research Council Grants ProtistWorld (PI P.L.-G., Grant Agreement no. 322669) and CALCYAN (PI K.B., Grant Agreement no. 307110) under the European Union's Seventh Framework Program and the RTP Génomique environnementale of the CNRS (project MetaStrom, PI D.M.).

References

Altermann, W., Kazmierczak, J., Oren, A. & Wright, D. T. (2006). Cyanobacterial calcification and its rock-building potential during 3.5 billion years of Earth history. *Geobiol* **4**, 147-166.

Amarouche-Yala, S., Benouadah, A., El Ouahab Bentabet, A. & López-García, P. (2014). Morphological and phylogenetic diversity of thermophilic cyanobacteria in Algerian hot springs. *Extremophiles* **18**, 1035-1047.

Arp, G., Reimer, A. & Reitner, J. (2001). Photosynthesis-induced biofilm calcification and calcium concentrations in Phanerozoic oceans. *Science* **292**, 1701-1704.

Benzerara, K., Skouri-Panet, F., Li, J. & other authors (2014). Intracellular Ca-carbonate biomineralization is widespread in cyanobacteria. *Proc Natl Acad Sci U S A* **111**, 10933-10938.

Buick, R. (2008). When did oxygenic photosynthesis evolve? *Philos Trans R Soc Lond B Biol Sci* **363**, 2731-2743.

Castenholz, R. W. (2001). General characteristics of the cyanobacteria. In Bergey's Manual of Systematic Bacteriology, pp. 474-487. Edited by D. R. Boone & R. W. Castenholz. New York: Springer.

Couradeau, E., Benzerara, K., Moreira, D., Gérard, E., Kazmierczak, J., Tavera, R. & López-García, P. (2011). Prokaryotic and eukaryotic community structure in field and cultured microbialites from the alkaline Lake Alchichica (Mexico). *PLoS One* **6**, 14.

Couradeau, E., Benzerara, K., Gérard, E., Moreira, D., Bernard, S., Brown, G. E., Jr. & López-García, P. (2012). An early-branching microbialite cyanobacterium forms intracellular carbonates. *Science* **336**, 459-462.

Gray, M. W. & Doolittle, W. F. (1982). Has the endosymbiont hypothesis been proven? *Microbiol Rev* **46**, 1-42.

Head, I. M., Gray, N. D., Clarke, K. J., Pickup, R. W. & Jones, J. G. (1996). The phylogenetic position and ultrastructure of the uncultured bacterium *Achromatium oxaliferum*. *Microbiology* **142**, 2341-2354.

Kamennaya, N. A., Ajo-Franklin, C. M., Northen, T. & Jansson, C. (2012). Cyanobacteria as biocatalysts for carbonate mineralization. *Minerals* **2**, 338-364.

Lau, M. C., Aitchison, J. C. & Pointing, S. B. (2009). Bacterial community composition in thermophilic microbial mats from five hot springs in central Tibet. *Extremophiles* **13**, 139-149.

Li, J., Margaret Oliver, I., Cam, N. & other authors (2016). Biomineralization patterns of intracellular carbonatogenesis in cyanobacteria: Molecular hypotheses. *Minerals* **6**, 10.

McNeill, J., Barrie, F. R., Buck, W. R. & other authors (2012). International Code of Nomenclature for algae, fungi, and plants (Melbourne Code) Regnum Vegetabile 154: Koeltz Scientific Books.

Obst, M., Wehrli, B. & Dittrich, M. (2009). $CaCO_3$ nucleation by cyanobacteria: laboratory evidence for a passive, surface-induced mechanism. *Geolbiol* **7**, 324-347.

Porta, D., Rippka, R. & Hernandez-Marine, M. (2000). Unusual ultrastructural features in three strains of *Cyanothece* (cyanobacteria). *Arch Microbiol* **173**, 154-163.

Ragon, M., Benzerara, K., Moreira, D., Tavera, R. & López-García, P. (2014). 16S rDNA-based analysis reveals cosmopolitan occurrence but limited diversity of two cyanobacterial lineages with contrasted patterns of intracellular carbonate mineralization. *Front Microbiol* **5**, 331.

Riding, R. (2006). Cyanobacterial calcification, carbon dioxide concentrating mechanisms, and Proterozoic-Cambrian changes in atmospheric composition. *Geobiol* **4**, 299-316.

Rippka, R., Waterbury, J. & Cohen-Bazire, G. (1974). A cyanobacterium which lacks thylakoids. *Arch Microbiol* **100**, 419-436.

Saghai, A., Zivanovic, Y., Zeyen, N. & other authors (2015). Metagenome-based diversity analyses suggest a significant contribution of non-cyanobacterial lineages to carbonate precipitation in modern microbialites. *Front Mirobiol* **6**, 797.

Saw, J. H., Schatz, M., Brown, M. V. & other authors (2013). Cultivation and complete genome sequencing of *Gloeobacter kilaueensis* sp. nov., from a lava cave in Kilauea Caldera, Hawai'i. *PLoS One* **8**, e76376.

Shi, L., Cai, Y., Li, P., Yang, H., Liu, Z., Kong, L., Yu, Y. & Kong, F. (2009). Molecular identification of the colony-associated cultivable bacteria of the cyanobacterium *Microcystis aeruginosa* and their effects on algal growth. *J Freshwater Ecol*, 211-218.

Turner, S., Pryer, K. M., Miao, V. P. & Palmer, J. D. (1999). Investigating deep phylogenetic relationships among cyanobacteria and plastids by small subunit rRNA sequence analysis. *J Eukaryot Microbiol* **46**, 327-338.

Figure legends

Fig. 1. Differential interference contrast (DIC) image of several Alchichica-D10 cells collected from an aquarium biofilm. Bar, 10 µm.

Fig. 2. Electron microscopy analyses of Alchichica-D10 cells grown in BG11. (a) Scanning-transmission electron microscopy image in high angle annular dark field (STEM-HAADF) mode: Ca-carbonates appear as brighter round-shaped inclusions, while polyphosphate granules are darker, sometimes bigger globules. (b) Scanning-transmission electron microscopy energy dispersive X-rays spectrometry (STEM-EDX) map of the same area: Calcium is in red, phosphorus in green and carbon in blue; as a result, Ca-carbonates appear in red and polyphosphate granules in green. Bars, 1 µm.

Fig. 3. Bright-field TEM image of a thin section of Alchichica-D10 cells embedded in EPON resin. Several concentric thylakoid membranes are visible under the cell membrane. Arrowheads indicate structures that may correspond to carboxysomes. Bar, 1 µm.

Fig. 4. Bayesian phylogenetic tree based on the analysis of a concatenation of 59 conserved proteins (7220 amino acids) reconstructed using PhyloBayes MPI (Lartillot *et al.*, 2013) with the CAT GTR model. Numbers at branches are posterior probabilities (only those >0.50 are shown). For space constraints, the outgroup and the *Synechococcus/Prochlorococcus* group have been replaced by triangles (for the complete tree see Fig. S6, available in the online Supplementary Material). The scale bar indicates the number of substitutions per position.

Figure 1

Figure 2

Click here to download Figure FIGURE 2.tif

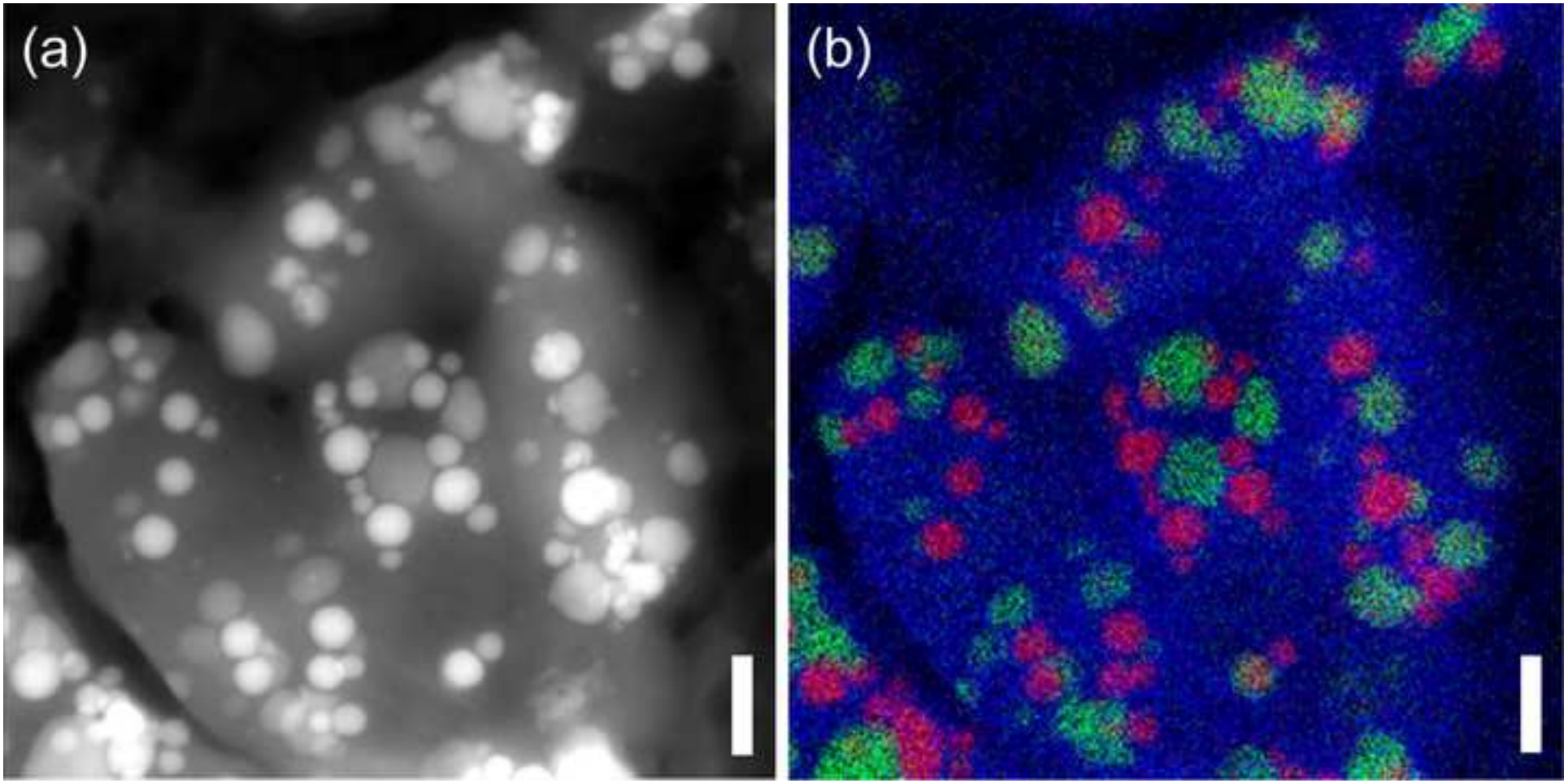

Figure 3

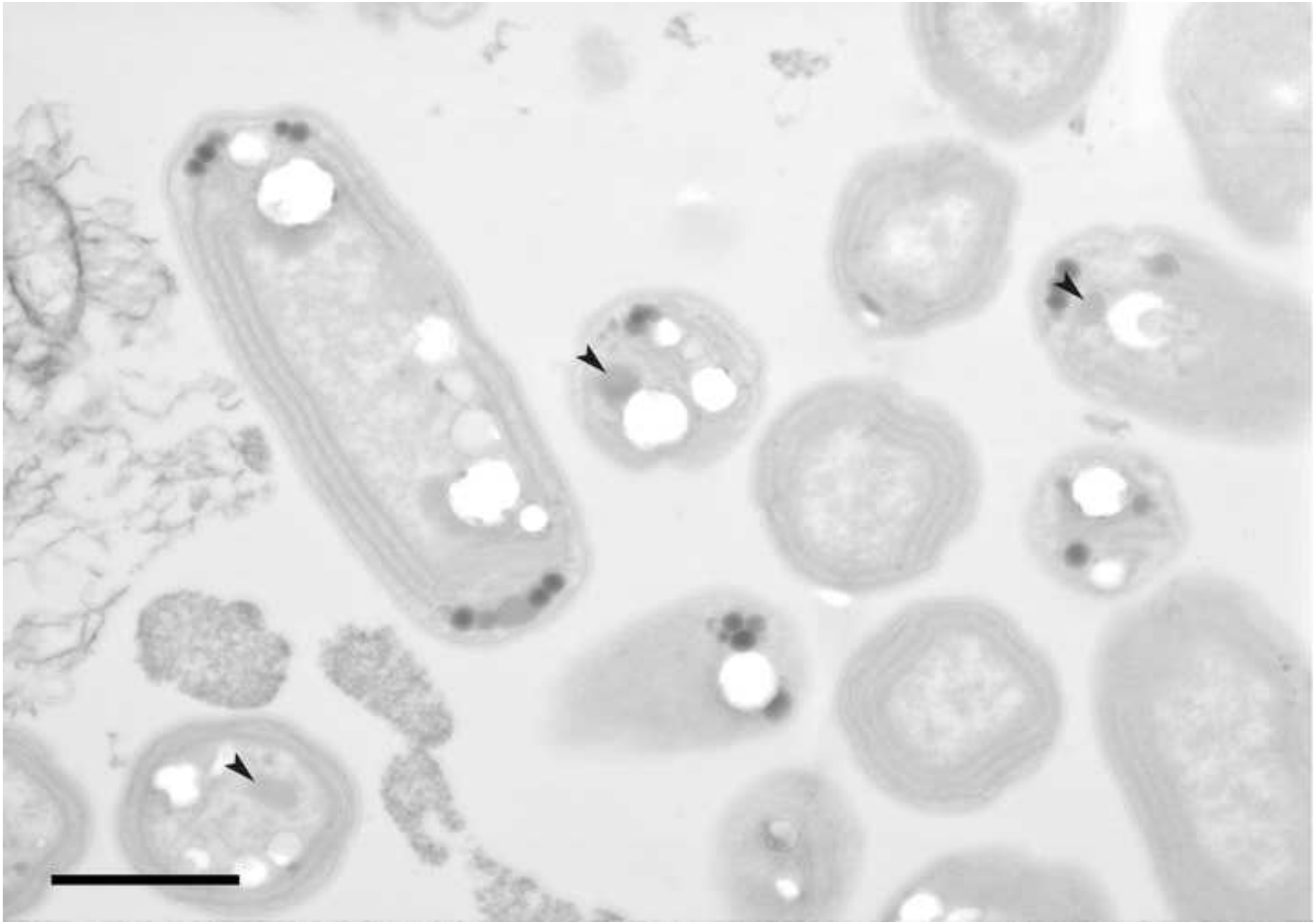

Figure 4

Click here to download Figure FIGURE 4.tif

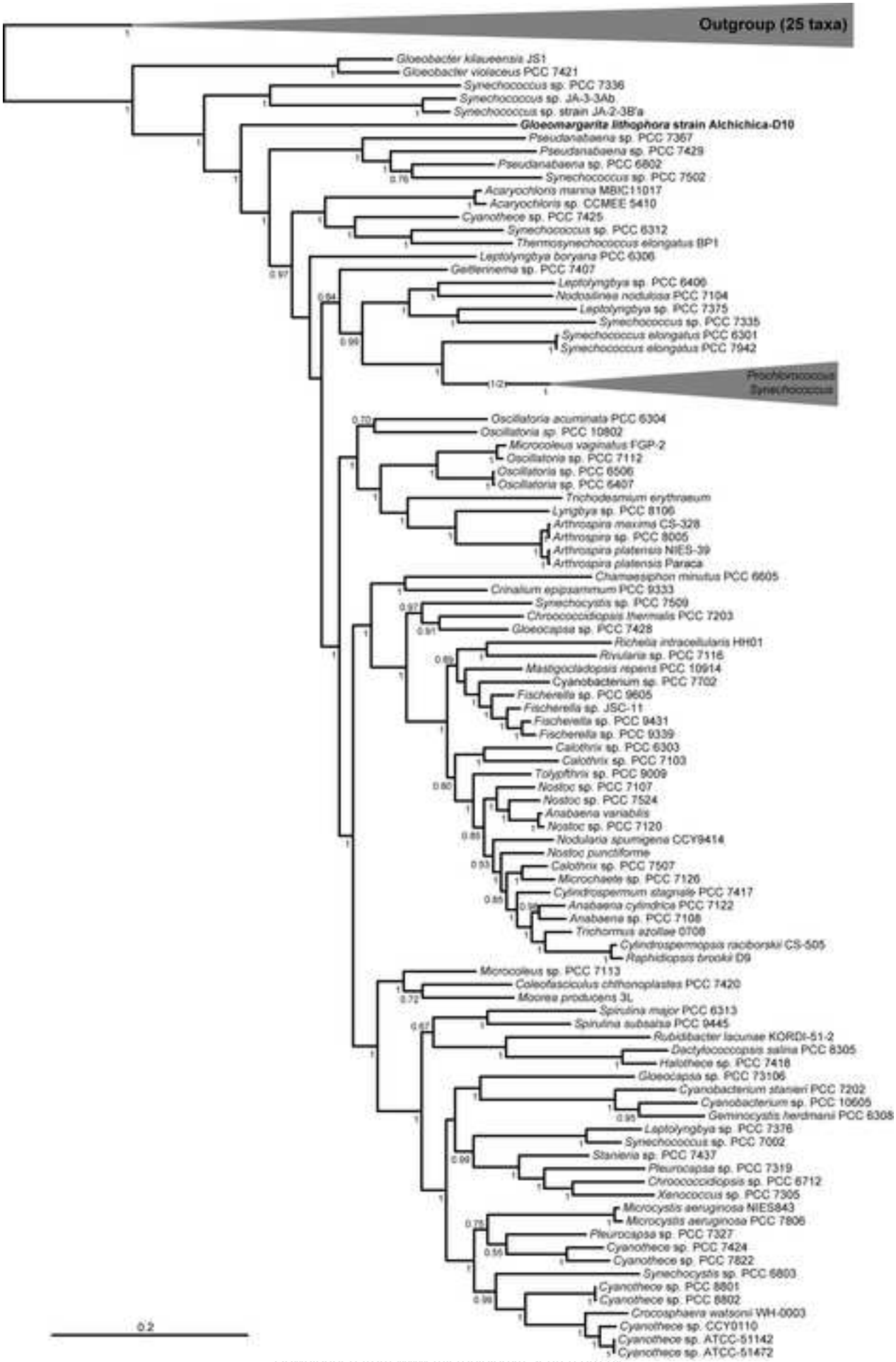

Supplementary Table S1, Proteins used for phylogenetic reconstruction

Protein	Protein name
EFG	elongation factor G
EFTs	elongation factor Ts
EFTu	elongation factor Tu
IF-1	initiation factor 1
IF-2B	initiation factor 2B
IF-3	initiation factor 3
rpL1	ribosomal protein L1
rpL10	ribosomal protein L10
rpL11	ribosomal protein L11
rpL13	ribosomal protein L13
rpL14	ribosomal protein L14
rpL15	ribosomal protein L15
rpL16	ribosomal protein L16
rpL17	ribosomal protein L17
rpL18	ribosomal protein L18
rpL19	ribosomal protein L19
rpL2	ribosomal protein L2
rpL20	ribosomal protein L20
rpL21	ribosomal protein L21
rpL22	ribosomal protein L22
rpL23	ribosomal protein L23
rpL24	ribosomal protein L24
rpL27	ribosomal protein L27
rpL28	ribosomal protein L28
rpL29	ribosomal protein L29
rpL3	ribosomal protein L3
rpL31P	ribosomal protein L31P
rpL32	ribosomal protein L32
rpL33	ribosomal protein L33
rpL34	ribosomal protein L34
rpL35	ribosomal protein L35
rpL4	ribosomal protein L4
rpL5	ribosomal protein L5
rpL6	ribosomal protein L6
rpL7-L12	ribosomal protein L7-L12
rpL9	ribosomal protein L9
rpPSRP3	ribosomal protein PSRP3
rpS10	ribosomal protein S10
rpS11	ribosomal protein S11
rpS12	ribosomal protein S12
rpS13	ribosomal protein S13
rpS14	ribosomal protein S14
rpS15	ribosomal protein S15
rpS16	ribosomal protein S16
rpS17P	ribosomal protein S17P
rpS18	ribosomal protein S18
rpS19	ribosomal protein S19
rpS1P	ribosomal protein S1P
rpS2	ribosomal protein S2

rpS20	ribosomal protein S20
rpS21	ribosomal protein S21
rpS3	ribosomal protein S3
rpS30EA	ribosomal protein S30EA
rpS4	ribosomal protein S4
rpS5	ribosomal protein S5
rpS6	ribosomal protein S6
rpS7	ribosomal protein S7
rpS8	ribosomal protein S8
rpS9	ribosomal protein S9

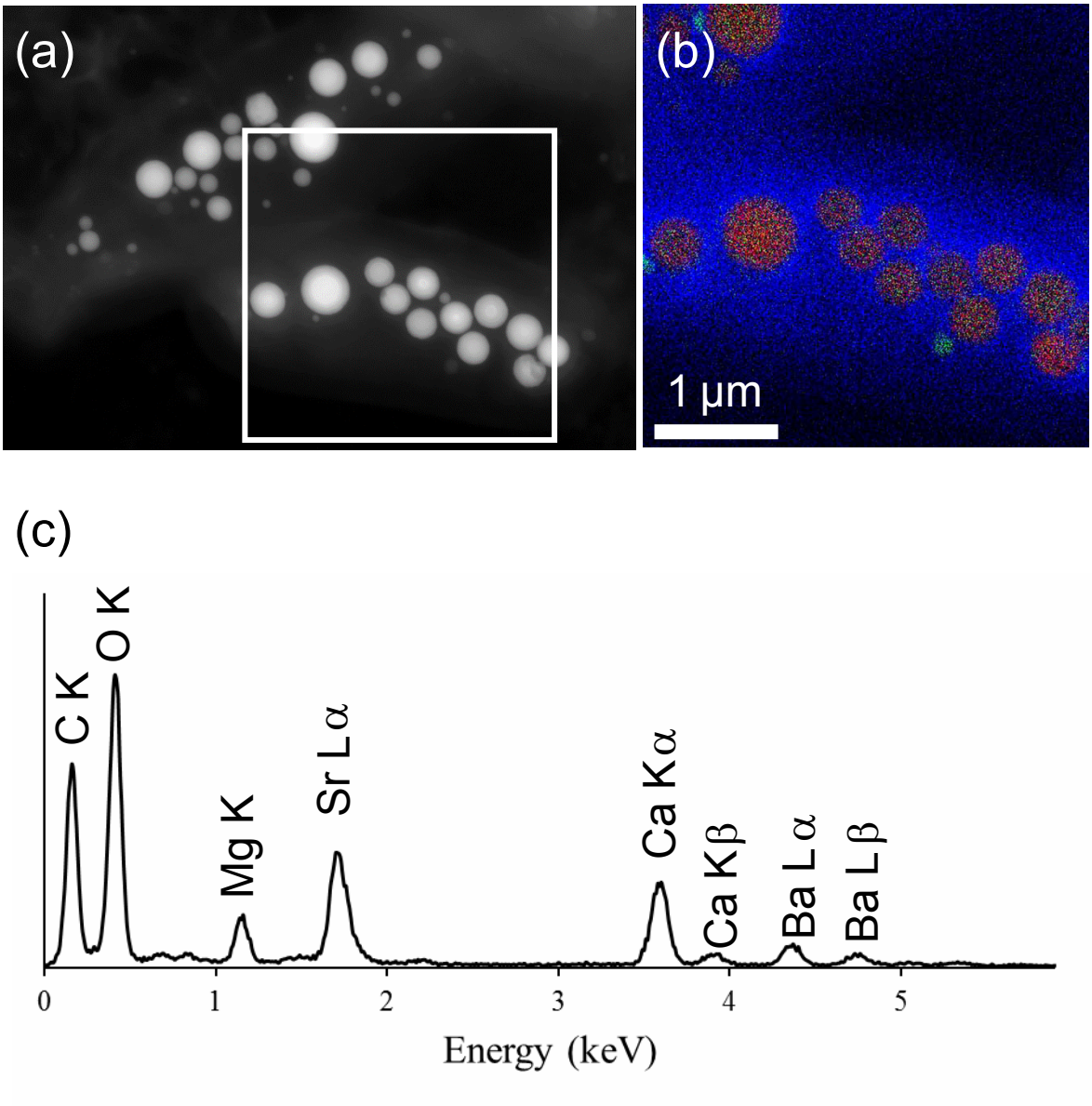

Supplementary Fig. S1. Electron microscopy analyses of Alchichica-D10 cells grown in aquarium water. (a) Scanning-transmission electron microscopy high angle annular dark field (STEM-HAADF) image: Ca-carbonates appear as brighter round-shaped inclusions. (b) Energy dispersive X-ray spectrometry (EDXS) map of the area outlined in (a): Calcium is in red, phosphorus in green and carbon in blue; as a result, Ca-carbonates appear in red and PolyP granules in green. (c) EDXS spectrum of a carbonate inclusion showing the presence of Ca, Sr, Mg and Ba.

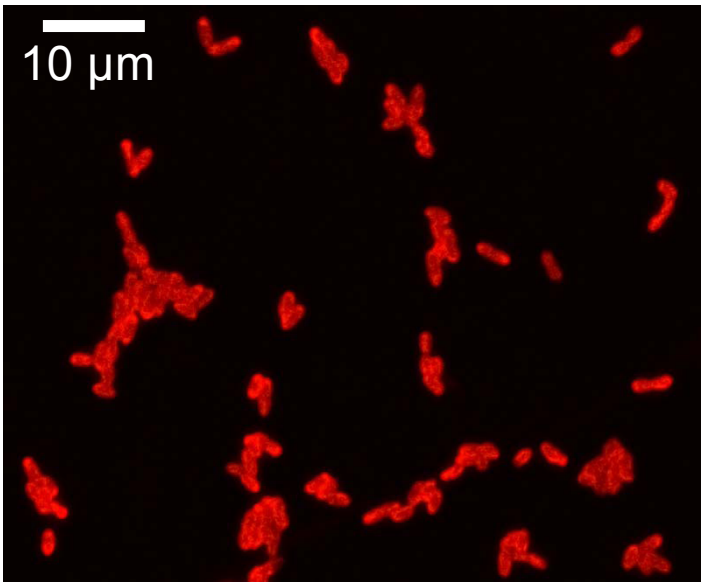

Supplementary Fig. S2. Autofluorescence of Alchichica-D10 cells observed under confocal laser scanning microscopy with UV light illumination (405 nm). Bar, 10 µm.

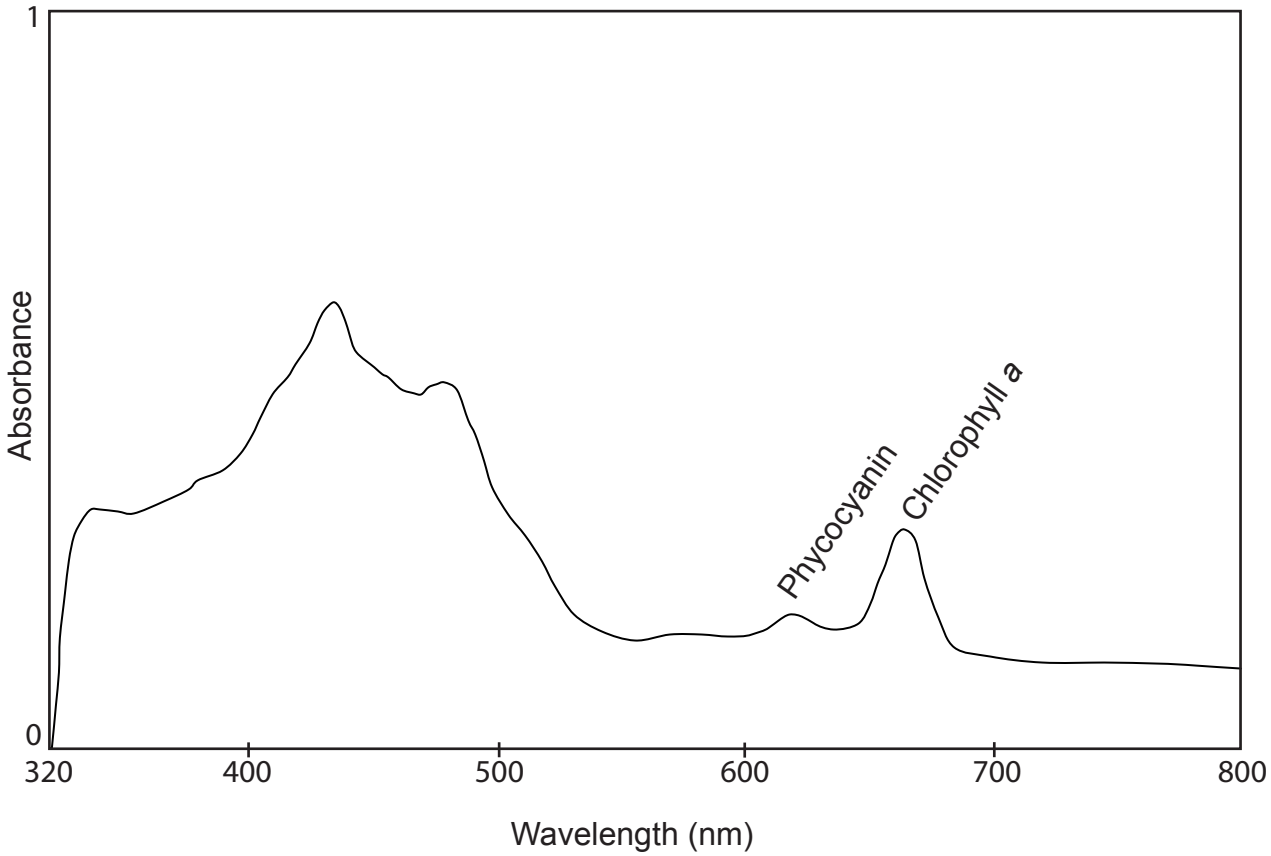

Supplementary Fig. S3. Absorption spectra of strain Alchichica-D10 pigments extracted with 90% acetone.

(a)

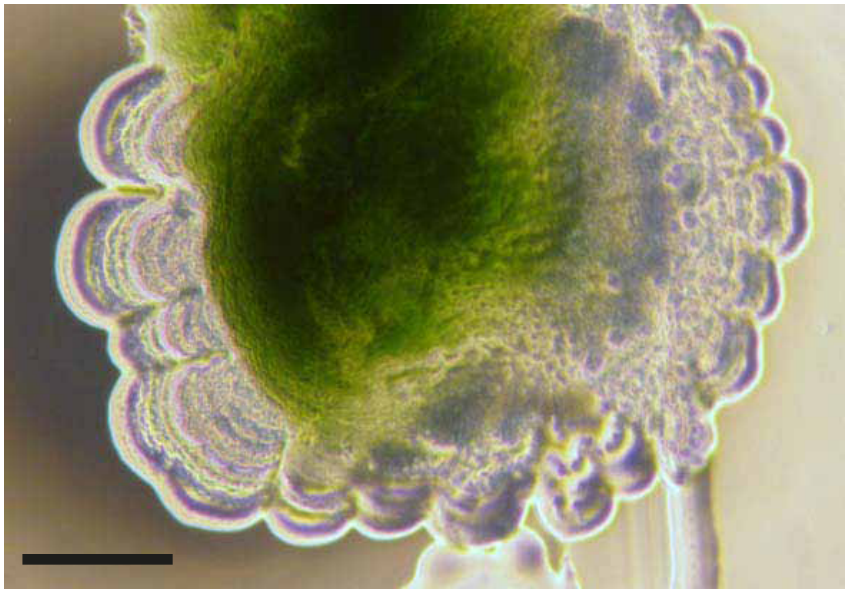

(b)

Supplementary Fig. S4. (a) Alchichica-D10 strain colony growing on a BG11-agar plate. (b) Magnification of the colony border. Bars, 1 mm (a) and 100 µm (b).

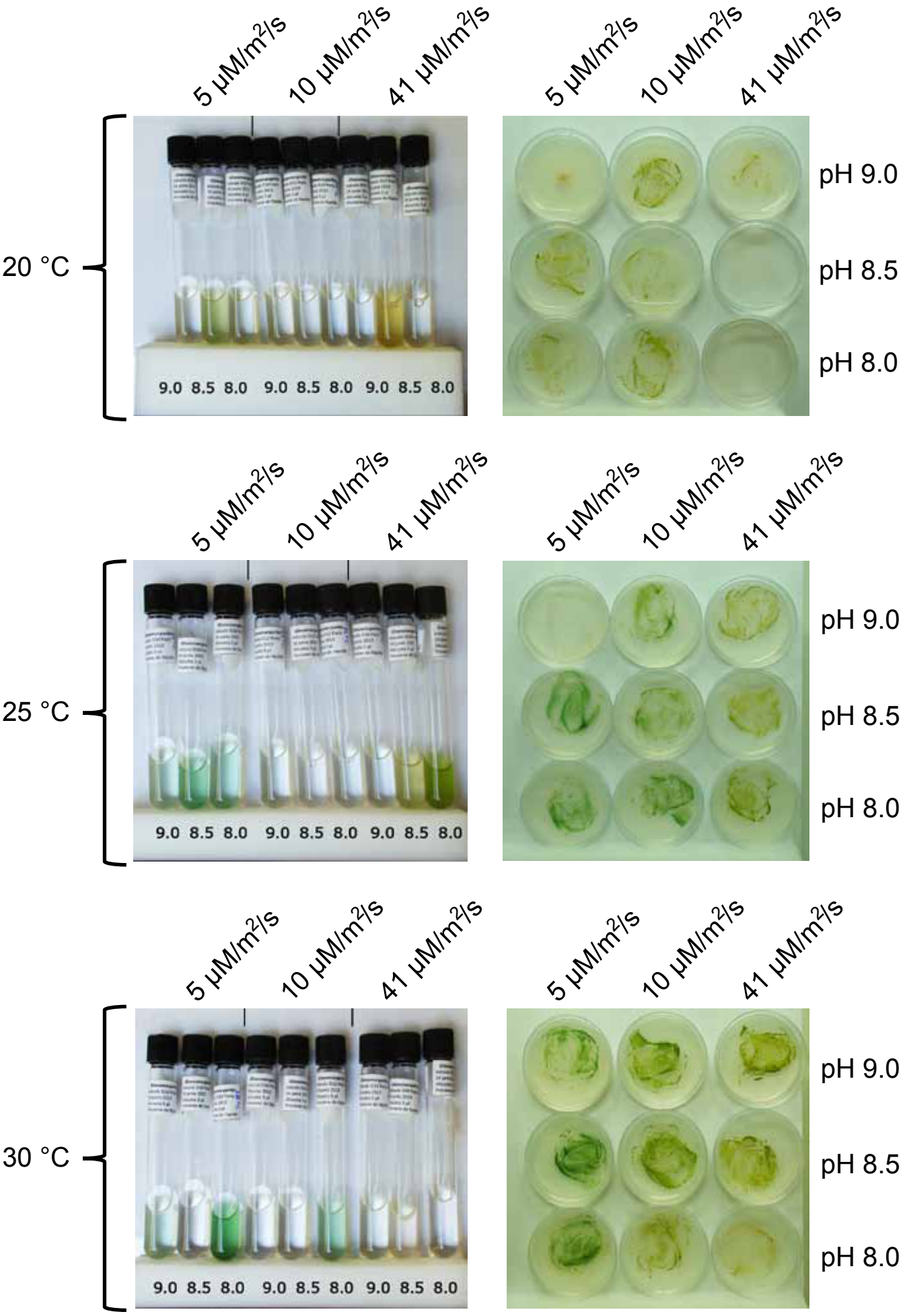

Supplementary Fig. S5. Growth of strain Alchichica-D10 in liquid and solid BG11 medium under different temperature, pH, and light intensity conditions.

Supplementary Fig. S6. Bayesian phylogenetic tree based on the analysis of a concatenation of 59 proteins (7220 amino acids) reconstructed using PhyloBayes MPI with the CAT GTR model. Numbers at branches are posterior probabilities (only those >0.50 are shown). The scale bar indicates the number of substitutions per position.